Gören, K., Bağlan, M., Yıldıko, Ü. (2024). Antimicrobial, and Antitubercular Evaluation with ADME and Molecular Docking Studies and DFT Calculatıons of (Z)-3-((1-(5-amino-1,3,4-thiadiazol-2-yl)-2-Phenylethyl)imino)-5-nitroindolin-2-one Schiff Base. *The Black Sea Journal of Sciences*, 14(4), 1694-1708.

The Black Sea Journal of Sciences, 14(4), 1694-1708, 2024. DOI: 10.31466/kfbd.1423367

KFBD

Karadeniz Fen Bilimleri Dergisi
The Black Sea Journal of Sciences
ISSN (Online): 2564-7377 https://dergipark.org.tr/tr/pub/kfbd

Araştırma Makalesi / Research Article

Antimicrobial, and Antitubercular Evaluation with ADME and Molecular Docking Studies and DFT Calculatıons of (Z)-3-((1-(5-amino-1,3,4-thiadiazol-2-yl)-2-Phenylethyl)imino)-5-nitroindolin-2-one Schiff Base

Kenan GÖREN[1*], Mehmet BAĞLAN[2], Ümit YILDIKO[3]

Abstract

(Z)-3-((1-(5-Amino-1,3,4-Thiadiazol-2-yl)-2-Phenylethyl)İmino)-5-nitroindolin-2-one Schiff Base compound (ATSB) have lately gained popularity, so the concept that these compounds should be researched has been highlighted. ATSB molecule, a unique Schiff base complex, was selected for molecular modeling research for publication in the literature. Initially, dependent density functional theory (DFT) computations were performed on ATSB molecule (geometry optimization, HOMO-LUMO, MEPS maps, dipole moment calculations, NBO analysis, and Mulliken Atomic Charges). Additionally, ADME analyzes have been carried out for the ATSB molecule and the color regions are given separately. Schiff bases have been shown to have an important role in antibacterial and antituberculosis medication illness and drug repair. Finally, in our investigation, molecular docking analysis ments were performed individually for ATSB molecule with two distinct enzymes (5V3X and 5V3Y), docking scores and receptor models have been given.

Keywords: Molecular Docking, DFT, MEP, NBO, ADME.

(Z)-3-((1-(5-amino-1,3,4-tiadiazol-2-il)-2-feniletil)imino)-5-nitroindolin-2-on Schiff Bazının DFT Hesaplamaları ADME ve Moleküler Doking ile Antimikrobiyal ve Antitüberküloz Değerlendirmesi

Öz

(Z)-3-((1-(5-Amino-1,3,4-Thiadiazol-2-il)-2-Feniletil)İmino)-5-nitroindolin-2-one Schiff Bazı bileşiği (ATSB) son zamanlarda popülerlik kazandığından bu bileşiklerin araştırılması gerektiği kavramı ön plana çıkmıştır. Eşsiz bir Schiff bazı kompleksi olan ATSB molekülü, literatürde yayınlanmak üzere moleküler modelleme araştırması için seçildi. İlk olarak ATSB molekülü üzerinde yoğunluk fonksiyonel teorisi (DFT) hesaplamaları (geometri optimizasyonu, HOMOLUMO, MEPS haritaları, dipol moment hesaplamaları, NBO analizi ve Mulliken atom yükleri) yapıldı. Aynı zamanda ATSB molekülü için ADME analizleri yapılmış olup, renk bölgeleri ayrı ayrı verilmiştir. Schiff bazlarının antibakteriyel ve antitüberküloz ilaç hastalıkları ve ilaç onarımında önemli bir role sahip olduğu gösterilmiştir. Son olarak araştırmamızda ATSB molekülü için ayrı ayrı iki farklı enzim (5V3X and 5V3Y) ile moleküler kenetlenme analizleri yapıldı ve kenetlenme skorları ve reseptör modelleri verildi.

Anahtar Kelimeler: Moleküler Doking, DFT, MEP, NBO, ADME.

[1,2]Kafkas University, Department of Chemistry, Kars, Turkey, kenangoren49@gmail.com mehmetbaglan36@gmail.com
[3]Kafkas University, Department of Bioengineering, Kars, Turkey, yildiko1@gmail.com

[*]Sorumlu Yazar/Corresponding Author
Geliş/Received: 21.01.2024 **Kabul/Accepted:** 19.10.2024 **Yayın/Published:** 15.12.2024

1. Introduction

The Schiff base is a chemical which has a functional group with a -CHN bond formed by the the condensation process of a carbonyl molecule by amines. Anyls, imines, and azomethines are other names for them (da Silva et al., 2011). Schiff bases, which are made up of a unique molecular framework, have piqued the scientific community's interest due to their extensive uses in a variety of sectors (Hodnett & Dunn, 1970). Due to their synthetic flexibility, extensive structure functions, synthetic sensitivity to diverse actions, existence of (-CHN) imine group, and chelating properties, Schiff bases have particularly important (Cordes & Jencks, 1962). Schiff bases are among the most important pharmacologically chemical compounds, with a wide range of physiological and biological characteristics including analgesic, antimalarial, antiasthmatic, antituberculosis, antiviral, antioxidant, anticonvulsant, antihypertensive, antidiabetic, and so on (Metzler et al., 1980). When Schiff bases coordinate with metal ions, these physiological features are amplified. Computational analysis, like all synthetic chemistry, has become a potent tool to researching chemical events including the structures and behavior of molecular elements employing computers. It is also crucial in establishing the features of the molecular framework under investigation (Wang et al., 2021). Molecular docking is an essential modeling tool that exposes how a drug operates in the body by exposing the drug's compatibility with the protein, binding force, and binding capacity for the protein (Morris & Lim-Wilby, 2008). Density Functional Theory (DFT) is emerging as a valuable method for obtaining vital information about the stability and action of freshly manufactured medicines (Bagayoko, 2014). These theoretical predictions are far more essential in predicting probable non-covalent interactions between produced compounds, since these interactions improve the bioactivity of potential bioactive compounds. As a result, computational studies aid in the development of better chemical compounds for high-performance biomedical applications. Mycobacterium tuberculosis is an airborne bacteria that causes tuberculosis (TB), which affects over ten million people and kills over one million each year. Antimicrobial and antituberculosis drug development and discovery is one of the most difficult study areas in the scientific community due to the inadequate efficacy and inadequacy of pharmacological alternatives in today's treatment conditions, long treatment periods, toxicity, high cost, and resistance (Prasad et al., 2022). Methods for predicting a protein's 3D structure are classified into three types: de novo modeling or ab initio, filamentation, and comparative modeling or homology. For determining the actual multiple of a transmitted sequence, ab initio modeling employs statistical analysis as well as a physics-based energy function (Rodney et al., 2017). When a suitable template is unavailable or the query is common, ab initio modeling is recommended to anticipate the form of a sequence. Despite sequence similarities, a particular fold

from the expected template is used. For folding prediction, many ab initio techniques employ statistical information, secondary structure, and fragment assembly. To keep the prediction issue tractable, all methods use a basic representation of the protein. More information on various ab initio estimating methodologies is provided to the reader (Taylor et al., 2001).

In this work, molecular modeling investigations of a single ATSB molecule were performed. DFT analyses were performed to learn more about the compound's energy characteristics and nonlinear optical characteristics. Moreover, ADME study has been undertaken to explore the compound's ADME characteristics. At last, molecular docking investigations have been conducted effectively to assess if the chemical ATSB molecule is consistent with the drug design phenomena. Each calculation (HOMO and LUMO analysis, geometry optimization, dipole moment and Mulliken Atomic Charges, MEP analysis) was calculated using the B3LYP/6-311G and MPW1PW9/6-31G methods. The precise binding location and binding process of ligand-protein connections were investigated using molecular docking.

2. Materials and Methods

For DFT calculations, ATSB molecule originally drawned in ChemBioDraw in the Gaussian 09 software. The drawned molecule was imported into Chem3D's GaussView 6.0. B3LYP/6-311G and MPW1PW9/6-31G base sets were used for DFT research (Michael J. Frisch, 2016), and pictures of each computation (HOMO and LUMO analysis, geometry optimization, Mulliken atomic charges and MEP analysis, dipole moment) have been calculated. Schrödinger's Maestro Molecular Modeling platform (version 11.8) was used to examine the precise binding location and binding process of ligand-protein associations. ADME analysis was performed using online servers like SwissADME (http://www.swissadme.ch/index.php). In the molecular docking strategy, the LLC model was used. As in prior investigations, all compounds were outfitted with the Ligprep module. The glide docking program was utilized to conduct ligand protein docking analysises. The highest binding energies and configurations were predicted between ligands and enzymes. The strongest binding affinities have been found at the lowest energy locations. The Discovery Studio 2016 client (Visualizer 2005) was used to visualize the molecular docking investigation.

3. Results and Discussion

3.1. Structure Details and Analysis

The geometry of a molecule is connected to the bond angle and bond length between its atoms and is one of the most critical parameters that directly determines the magnitude of the molecule's dipole moment (Bağlan, Gören, et al., 2022). The ideal bond length and bond angle characteristics of the molecule were obtained utilizing the B3LYP/6-311G-MPW1PW9/6-31G basic set and methods in the ATSB molecule DFT approach. B3LYP/6-311G-MPW1PW9/6-31G values are nearly identical. This signifies that the structure has the least amount of potential energy. The researchers compared two optimized sets of fundamental ATSB molecule. Every one bond lengths and angles in their aromatic rings are inside the normal range. In our molecule, large deviations in bond length appeared at atoms C11-C13 (1.49441 Å), C12-C32 (1.51525 Å), C16-S17 (1.83815 Å) and S17-C13 (1.86977 Å). Large deviations were observed in the trihedral structures of our molecule with bond angles of C3-C4-N7 (130.46994º), C9-C8-O19 (130.23347º) and C6-C5-C9 (133.13848º). In tetrahedral structures, a large change in the bond angles between C2-C3-C4-N7 (179.85928º), C13-S17-C16-N18 (-179.73213º) and N10-C11-C12-C32 (-169.18680º) atoms was observed.

Table 1. Theoretically calculated bond lengths (Å) and bond angles (º) to ATSB molecule

Bond Lengths	**B3LYP/ 6-311G**	**MPW1PW9/ 6-31G**	**Bond Lengths**	**B3LYP/ 6-311G**	**MPW1PW9/ 6-31G**
C1-N20	1.45620	1.44751	**C13-S17**	1.86977	1.84314
C4-N7	1.38283	1.37603	**N14-N15**	1.39549	1.38036
C4-C5	1.43428	1.43043	**S17-C16**	1.83815	1.81754
C8-O19	1.25943	1.25495	**N15-C16**	1.31574	1.31455
C8-C9	1.45838	1.45541	**C16-N18**	1.35367	1.34733
C9-N10	1.35980	1.35293	**C34-H38**	1.08264	1.08531
C11-N10	1.48386	1.47259	**C12-H28**	1.09240	1.09570
C12-C32	1.51525	1.50872	**N10-H43**	1.00902	1.00899
C11-C13	1.49441	1.48982	**N7-H26**	1.00482	1.00443
C13-N14	1.29424	1.29440	**C3-H24**	1.08061	1.08221
Bond Angles	**B3LYP/ 6-311G**	**MPW1PW9/ 6-31G**	**Bond Angles**	**B3LYP/ 6-311G**	**MPW1PW9/ 6-31G**
C3-C4-N7	130.46994	130.32175	**C9-C8-O19**	130.23347	130.27366
C1-N20-O21	118.30576	118.12177	**C12-C11-C13**	114.09990	113.78713
C1-N20-O22	118.47422	118.29519	**C13-S17-C16**	83.81664	84.28053
C6-C5-C9	133.13848	133.20431	**N14-N15-C16**	113.20826	113.10800
C5-C9-N10	126.59348	126.69889	**S17-C16-N18**	121.99408	122.11109
Planar Bond Angles	**B3LYP/ 6-311G**	**MPW1PW9/ 6-31G**	**Planar Bond Angles**	**B3LYP/ 6-311G**	**MPW1PW9/ 6-31G**
C2-C3-C4-N7	179.85928	179.92897	**N10-C11-C12-C32**	-169.18680	-170.91718
C2-C1-N20-O22	0.26523	0.34424	**N10-C11-C13-S17**	-68.94767	-69.81772
O19-C8-C9-N10	-1.21295	-1.27452	**C13-S17-C16-N18**	-179.73213	-179.84714
N10-C11-C13-N14	109.48722	108.36242	**N14-N15-C16-N18**	179.51880	179.61889

3.2. HOMO and LUMO Analysis

The highest occupied molecular orbital (HOMO), the lowest unoccupied molecular orbital (LUMO), and energy gaps have the primary electrical properties associated to orbitals in a structure. HOMOs are the orbital electrons with the greatest energy that can function as electron donors (Bağlan,

Gören, et al., 2023b). LUMO is the lowest energy orbital with adequate room to take electrons and can operate like an electron acceptor (Suhasini et al., 2015). The molecule interacts with different organisms is determined by the LUMO and HOMO orbitals. Figures 1 and 2 demonstrate the orbital representations of HOMO and LUMO using the same approach and settings as for the density ATSB molecule. E_{HOMO} -5.3602 eV, E_{LUMO} -2.9869 eV was determined using the B3LYP/6-311G basis set and technique. E_{HOMO} was estimated as -5.4490 eV, E_{LUMO} -2.6293 eV using the MPW1PW9/6-31G basis set and technique. The molecule's interactions with other species are determined by its HOMO and LUMO orbitals (Demir & Akman, 2017). It also aids in the determination of band discrepancy, chemical reactivity, and kinetic persistence. A tiny border shows a molecule's electronegativity, hardness, polarization, and other reactivity indices (Yildiko et al., 2021). Table 2 shows the chemical reactivity indices of our structure calculated using the same fundamental set procedures.

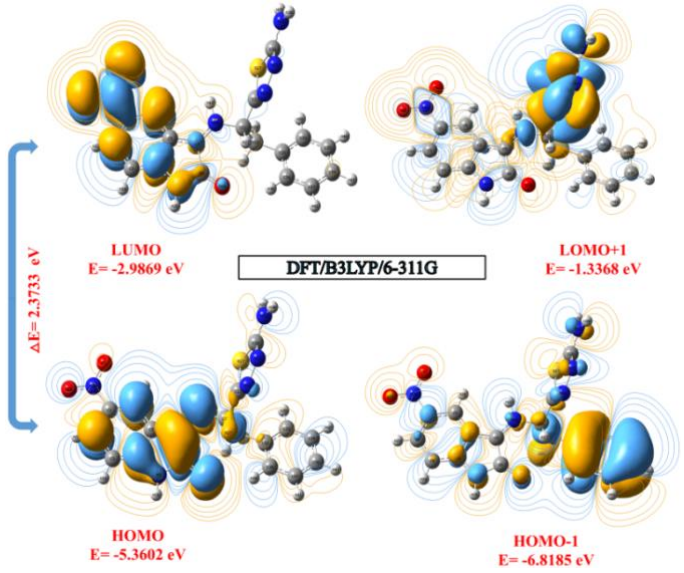

Figure 1. The boundary molecular orbitals of the ATSB molecule at the DFT/B3LYP/6-311G level

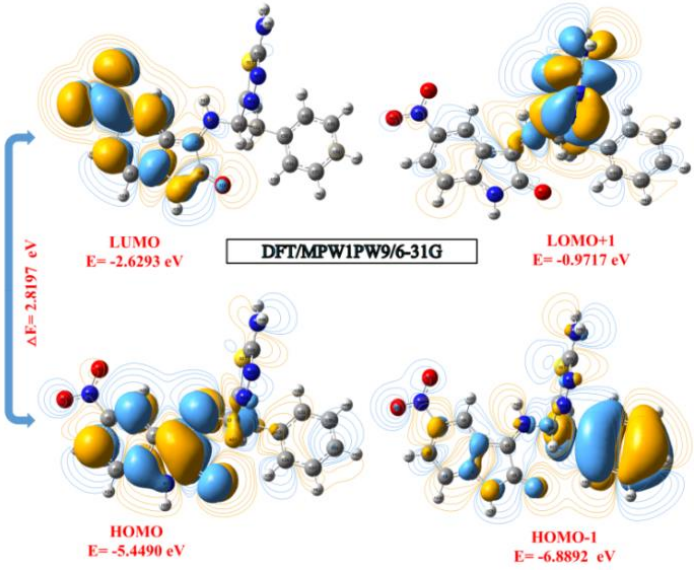

Figure 2. The boundary molecular orbitals of the ATSB molecule at the DFT/MPW1PW9/6-31G level

Table 2. Calculated quantum chemical parameters*(in eV) to low energy compatibilities with B3LYP/6-311G-MPW1PW9/6-31G methods of the ATSB molecule

Molecules Energy		B3LYP/ 6-311G	MPW1PW9/ 6-31G
E_{LUMO}		-2.9869	-2.6293
E_{HOMO}		-5.3602	-5.4490
E_{LUMO+1}		-1.3368	-0.9717
E_{HOMO-1}		-6.8185	-6.8892
Energy Gap	$(\Delta E)\|E_{HOMO}\text{-}E_{LUMO}/$	2.3733	2.8197
Ionization Potential	$(I=-E_{HOMO})$	5.3602	5.4490
Electron Affinity	$(A=-E_{LUMO})$	2.9869	2.6293
Chemical hardness	$(\eta=(I-A)/2)$	1.1866	1.4098
Chemical softness	$(s=1/2\eta)$	0.5933	0.7049
Chemical Potential	$(\mu=-(I+A)/2)$	-4.1735	-4.0391
Electronegativity	$(\chi=(1+A)/2)$	1. 9934	1.8146
Electrophilicity index	$(\omega=\mu^2/2\eta)$	7.3393	5.9356

3.3. Mulliken Atomic Charges

Mulliken Atomic Charges must be calculated in order to use quantum chemical computations effectively (Bağlan, Gören, et al., 2023a). It has been discovered that certain C atoms have positive and others have negative. Using DFT/MPW1PW9/6-31G basis set and method, a) Structure Optimization, b) Bond Lengths, c) Mülliken Charge d) Atomic Mass have been given in Figure 3. Figure 4 shows a graph comparing Mulliken atomic charges for ATSB molecule.

Table 3. Mulliken Atomic Charges of the ATSB molecule

ATOMS	B3LYP/ 6-311G	MPW1PW9/ 6-31G	ATOMS	B3LYP/ 6-311G	MPW1PW9/ 6-31G
C1	0.213	0.272	**N7**	-0.839	-0.867
C2	-0.132	-0.172	**N10**	-0.717	-0.759
C3	-0.059	-0.134	**N14**	-0.138	-0.204
C4	0.358	0.345	**N15**	-0.205	-0.250
C6	0.044	-0.109	**S17**	0.288	0.475
C8	0.504	0.543	**N18**	-0.722	-0.752
C9	0.274	0.268	**O19**	-0.380	-0.453
C11	-0.083	-0.031	**N20**	0.030	0.077
C12	-0.441	-0.373	**O21**	-0.276	-0.312
C13	-0.068	-0.116	**O22**	-0.271	-0.308
C32	0.012	0.064	**H23**	0.199	0.225
C33	-0.121	-0.185	**H24**	0.175	0.193
C34	-0.118	-0.190	**H25**	0.201	0.223
C35	-0.169	-0.169	**H26**	0.352	0.362
C37	-0.163	-0.169	**H27**	0.276	0.275
C39	-0.125	-0.160	**H28**	0.176	0.171

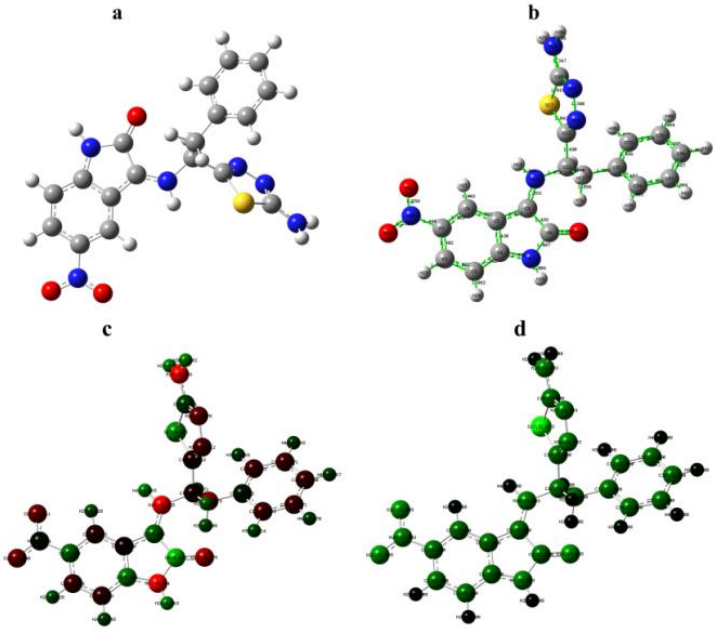

Figure 3. Molecule with DFT/MPW1PW9/6-31G basis set ATSB molecule a) Structure Optimization, b) Bond Lengths, c) Mülliken Charge d) Atomic Mass

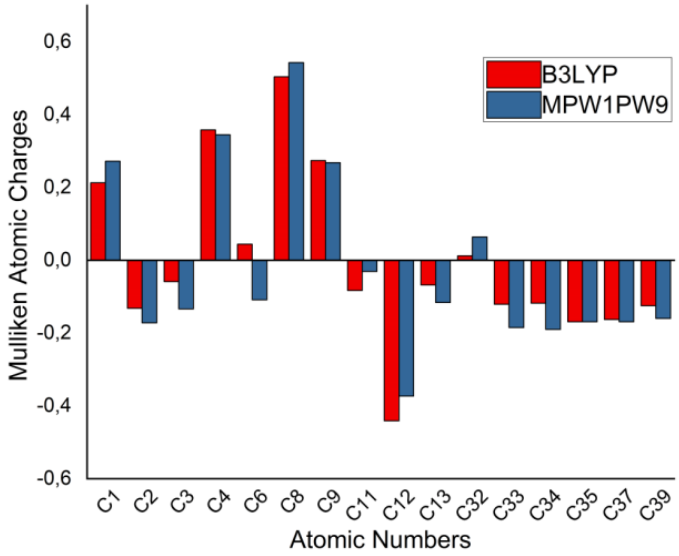

Figure 4. Mulliken atomic charge comparison for ATSB molecule

3.4. Molecular Electrostatic Potential (MEP)

The surface of molecule electrostatic potential MEPS depicts the molecule's electrostatic potential values and shape, size, has been displayed to ATSB molecule (Bağlan, Yildiko, et al., 2023). MEPS mapping is extremely helpful in determining the physicochemical features of a structure in molecules. The color green denotes a neutral electrostatic potential (Lakshminarayanan et al., 2021). As indicated in Figure 5, MEPS maps are mapped for ATSB molecule. In the example of ATSB molecule, the MEPS map depicts negative potential areas surrounding nitrogen atoms in red. It has a nearly neutral potential since the majority of the aromatic ring area has been indicatesed by green.

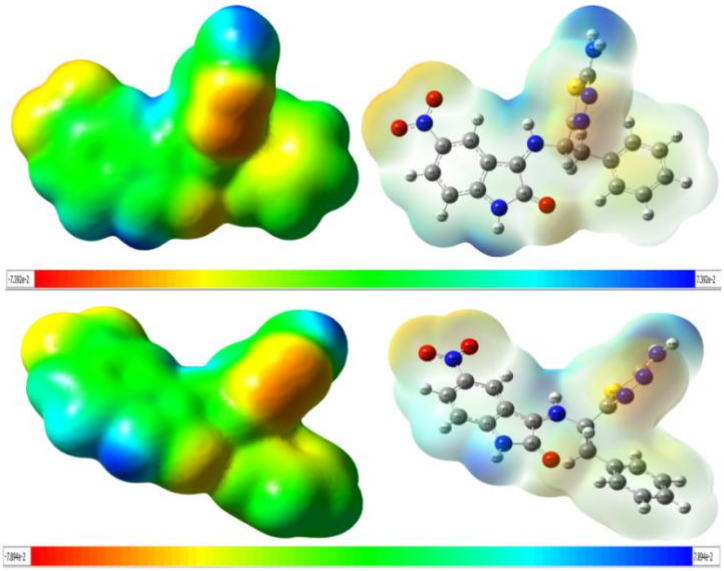

Figure 5. Molecular electrostatic potential surface of ATSB molecule using B3LYP/6-311G-MPW1PW9/6-31G basis sets and methods

3.5. Non-Linear Optical Properties (NLO)

The dipole moment is an essential feature of the energy related with the molecule's applied electric field. The dipole moment is made up of intermolecular interactions that involve Van der Waals type dipole-dipole forces, resulting in strong intermolecular attraction (Bhuiyan et al., 2011). The estimated values, total dipole moment and electronic dipole moment have been shown in Table 4. Nonlinear optical characteristics (NLO) are predicted computationally using polarizability (α) and hyperpolarizability (β). A material's hyperpolarizability influences the performance of its nonlinear optical properties. A molecule's polarizability, hyperpolarizability, and dipole moment must be strong for it to exhibit NLO properties, and the HOMO-LUMO energy difference must be small (Bağlan, Yildiko, et al., 2022). The polarization (α), hyperpolarization (β), and electric dipole moment (μ) of the ATSB molecule, NLO behavior have been measured using the B3LYP/6-311G-MPW1PW9/6-31G methods and bass sets. The computed NLO values are shown in Table 4. Equations (1-4) calculate the mean values of the x, y, and z components' total first static hyperpolarizability (β), static dipole moment (μ), and polarizability (α). The total values computed by the B3LYP/6-311G-MPW1PW9/6-31G methods for ATSB molecule are 3.53×10^{-30} esu and 3.57×10^{-30} esu, respectively.

$$\mu = (\mu_x^2 + \mu_z^2)^{1/2} \quad (1)$$

$$\alpha = 2^{-1/2}\left[(\alpha_{xx} - \alpha_{yy})^2 + (\alpha_{yy} - \alpha_{zz})^2 + (\alpha_{zz} - \alpha_{xx})^2 + 6\alpha_{xx}{}^2\right]^{1/2} \quad (2)$$

$$\beta_{Total} = (\beta^2 x + \beta^2 y + \beta^2 z)^{1/2} \quad (3)$$

$$= [(\beta xxx + \beta xyy + \beta xzz)^2 + (\beta yyy + \beta yxx + \beta yzz)^2 + (\beta zzz + \beta zxx + \beta zyy)^2]^{\frac{1}{2}} \quad (4)$$

Table 4. The dipole moments (Debye), polarizability (au), components, and total value of ATSB molecule calculated using B3LYP/6-311G-MPW1PW9/6-31G basis sets and methods

Parameters	B3LYP/ 6-311G	MPW1PW9/ 6-31G	Parameters	B3LYP/ 6-311G	MPW1PW9/ 6-31G
μ_x	1.8271	1.7539	β_{XXX}	217.8196	221.1544
μ_y	0.3411	0.2552	β_{YYY}	139.8053	137.3143
μ_z	-1.3873	-1.3865	β_{ZZZ}	-20.2750	-21.5576
$\mu_{(D)}$	2.3193	2.2503	β_{XYY}	49.4836	51.5710
α_{XX}	-193.6563	-190.2793	β_{XXY}	-147.7241	-155.1834
α_{YY}	-142.9606	-138.9960	β_{XXZ}	41.5721	41.1859
α_{ZZ}	-179.0606	-176.0950	β_{XZZ}	-28.5477	-25.4082
α_{XY}	34.9747	34.9276	β_{YZZ}	1.7935	0.8002
α_{XZ}	-16.3356	-16.5472	β_{YYZ}	39.1030	40.7312
α_{YZ}	-4.1660	-4.2169	β_{XYZ}	-18.0195	-17.5038
α (au)	-175.162	-174.744	**β (esu)**	3.53×10^{-30}	3.57×10^{-30}

3.6. NBO Analysis

The NBO approach evaluates occupied and empty orbital interactions, providing knowledge on both intramolecular and intermolecular reactions. In the NBO study of our chemical, a quadratic Fock matrix has been created to examine donor-acceptor reactions. The interaction results in a depart of occupancy from a localized NBO of the idealized Lewis structure to an empty non-Lewis orbital (Weinhold et al., 2016). The stability energy related to the displacement i-j to each donor (i) and acceptor (j) is approximated as E (2). NBO analysis has been used to determine charge transfer or charge displacement caused by intramolecular contact between bonds (Glendening et al., 2013). These are indicators of delocalization and hyperconjugation; the findings to ATSB molecule has been shown in Table 5.

Internal molecul interactions are manifested like a rise in electron density (ED) in antibody orbitals, resulting in the weakening of the appropriate bonds (C-O). The electron density (1.9938 au) of the conjugated substitution bond suggests a substantial dislocation, bond occupancy. It is higher than bonds, allowing for greater localization (Kurt et al., 2011). Table 5 shows how the intramolecular hyperconjugative interaction of the distribution of (C8-C9) electrons in the ring is caused by the stability of a section of the ring. *(N20-O11) and anti-Ring *(C8)-O19) stabilize around 24.76-2.25 kcal/mol. These values boosted conjugation resulting in substantial localisation.

Table 5. Selected NBO results of ATSB molecule calculated using the 6-31G basis set using the DFT/MPW1PW9 method

NBO(i)	Type	Occupancies	NBO(j)	Type	Occupancies	E(2)[a] (Kcal/mol)	E (j)-E(i)[b] (a.u.)	F (i, j)[c] (a.u)
C1-C6	π	0.80320	**N20-O21**	π*	0.34880	24.76	0.10	0.070
C2-C3	σ	0.98571	**C4-N7**	σ*	0.01446	3.36	1.06	0.075
C3-C4	σ	0.98822	**C4-C5**	σ*	0.01539	2.42	1.25	0.070
C4-C5	σ	0.98046	**C9-N10**	σ*	0.01000	2.81	1.24	0.075
C4-N7	σ	0.99160	**C8-O19**	σ*	0.11237	2.25	1.31	0.069
C5-C6	σ	0.98434	**C1-N20**	σ*	0.03768	2.23	1.03	0.061
N15-C16	π	0.94719	**C13-N14**	π*	0.13491	6.99	0.32	0.063
N20-O21	π	0.99172	**N20-O21**	π*	0.34880	4.60	0.24	0.052
C5-C9	σ	0.99172	**N10-C11**	σ*	0.02170	2.41	0.97	0.061
C32-C33	π	0.83279	**C35-C39**	π*	0.16511	10.40	0.28	0.068
C34-C37	π	0.83122	**C32-C33**	π*	0.17630	10.81	0.28	0.069
C35-C39	π	0.83412	**C32-C33**	π*	0.17630	10.19	0.28	0.068
C8-C9	σ	0.98404	**C5-C6**	σ*	0.01259	2.44	1.16	0.067
C8-O19	σ	0.99657	**C9-N10**	σ*	0.09441	4.03	0.36	0.050
C13-N14	π	0.96861	**C9-N10**	π*	0.09441	1.12	0.01	0.010
C15-C16	π	0.94719	**C13-N14**	π*	0.13491	41.88	0.02	0.061
C9-N10	σ	0.99320	**C8-O19**	σ*	0.09441	3.23	0.34	0.043
C11-H27	σ	0.97674	**C13-S17**	σ*	0.06350	4.33	0.59	0.065
N20-O21	π	0.99172	**C1-C6**	π*	0.17839	7.97	0.18	0.065
C13-N14	π	0.96861	**N15-C16**	π*	0.19779	3.89	0.31	0.048
C13-S17	σ	0.98766	**C16-N18**	σ*	0.01175	2.30	1.07	0.063
C16-S17	σ	0.98749	**C11-C13**	σ*	0.01562	1.92	1.03	0.056
C32-C33	σ	0.98676	**C35-C39**	σ*	0.00851	10.40	0.28	0.068
C33-H36	σ	0.98977	**C32-C34**	σ*	0.01292	2.35	1.07	0.064
C34-C37	π	0.98872	**C35-C39**	π*	0.16511	10.45	0.28	0.068
C34-H38	σ	0.98914	**C32-C33**	σ*	0.17630	2.39	1.07	0.064
C35-C39	π	1.99062	**C34-C37**	π*	0.15754	10.11	0.28	0.068
C8-C9	σ	1.98165	**N10-H43**	σ*	0.00997	3.55	0.02	0.051

3.7. Molecular Docking Studies

Molecular docking is important for studying the interplay of binding modes at the molecular scale and investigating the process of ligand receptor binding. Molecular docking has been used to determine the protein complexes of these enzymes were discovered by searching the online resource RSCB protein database for 5V3X and 5V3Y. This investigation, which included one chemical and two enzyme sets, yielded two good docking scores (Table 6) (Jakhar et al., 2020). These ligands were docked ligands' receptor-selected binding sites and to corroborate the experimental findings. Molecular docking results for ATSB molecule Antimicrobial, and Antitubercular were obtained to the enzyme's catalytic active site, and the docking results were analyzed in terms of binding affinity and interaction mode. However, The 5V3Y enzyme has the greatest binding affinity score based on molecular structure. The structural similarity of the protein structure to the natural ligand increases this amount. Protein dynamics governs how proteins interact with a variety of derivatives to create complexes which could enhance or restrict their biological capabilities. The binding patterns have

been investigated to identify the inhibitory mechanisms following selecting the optimal posture in the complete ligand-enzyme docking investigation.

Table 6. Docking score of molecule (1) PDB: 5V3X and PDB: 5V3Y

Compound	Docking Score	
	(PDB: 5V3X)	(PDB: 5V3Y)
ATSB Molecule	-7.866	-8.780

Figure 6 Depicts the Molekül-5V3X docking study's 3D and 2D interaction. The binding affinity for Molekül-5V3X was determined to be -7.86 kcal/mol. HOH-1988 hydrogen bound water hydrogen bond attaches to nitroindoline in this bonding mechanism, while ASP-1644 (5.12 Å) binds to Traditional Hydrogen. Thiadiazole is bound by a bond. Nitroindoline is made up of nitrogen, toluene ASN-1640 (4.53 Å) carbon hydrogen bond, SER-1636 (5.08 Å) and PHE-1670 (5.24 Å). ALA-1667 (4.67 Å) Pi-Alkyl bonded to the center of the thiadiazole ring, and Pi-Pi stack attached to the core of the benzene ring. Figure 6 depicts the binding pattern to the core of the benzene ring and other interactions. HIS-1664, TYR-1674, and PHE-1585 are van der Waals bound hydrogen in our compound's bonding mechanism.

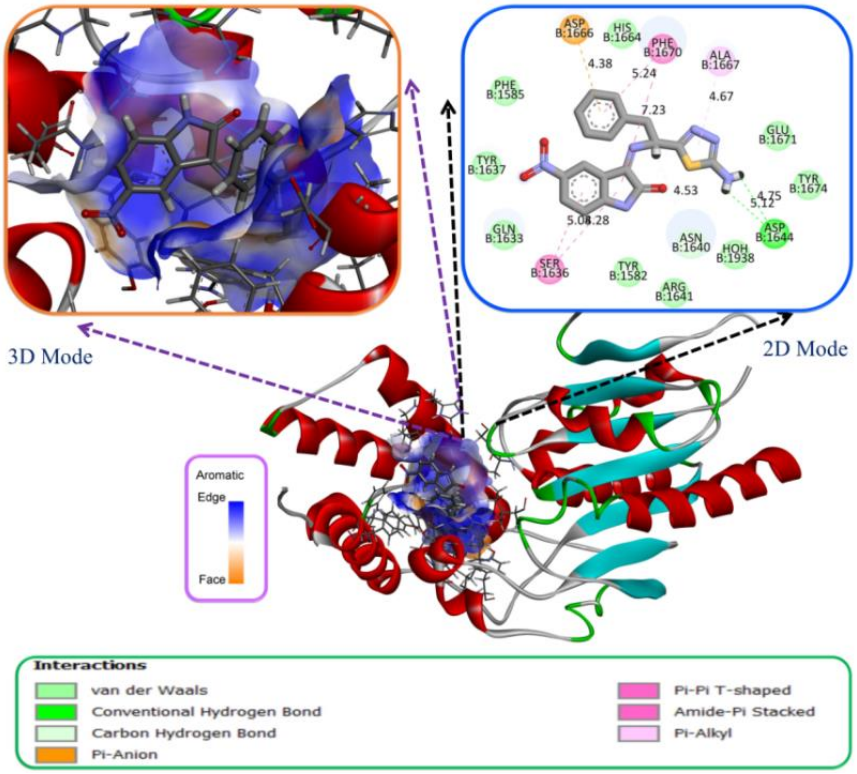

Figure 6. Molecule-5V3X mode of interaction with enzymes; 3D view of the donor/acceptor surface of aromatic bonds on the receptor and 2D view of ligand enzyme interactions

Figure 7, Molecule-5V3Y exhibits 3D and 2D interactions as a consequence the docking process. The maximum binding affinity score for molecule-5V3Y was -8.780 kcal/mol. ASN-1640 (5.74 Å) and ALA-1477 (4.33 Å) are normal hydrogen bonds connected to the sulfur and nitrogen of Thiadiazole, whereas PHE-1670 (4.94 Å) are benzene exchanges and core Pi-Pi connections of the stack, and ASP-1644 (5.83 Å). The nitrophenyl hydrogen is required for the pi-donor hydrogen bond to form. HIS-1664, TYR-1674, and ARG-1644 are van der Waals bound hydrogen in our compound's bonding mechanism.

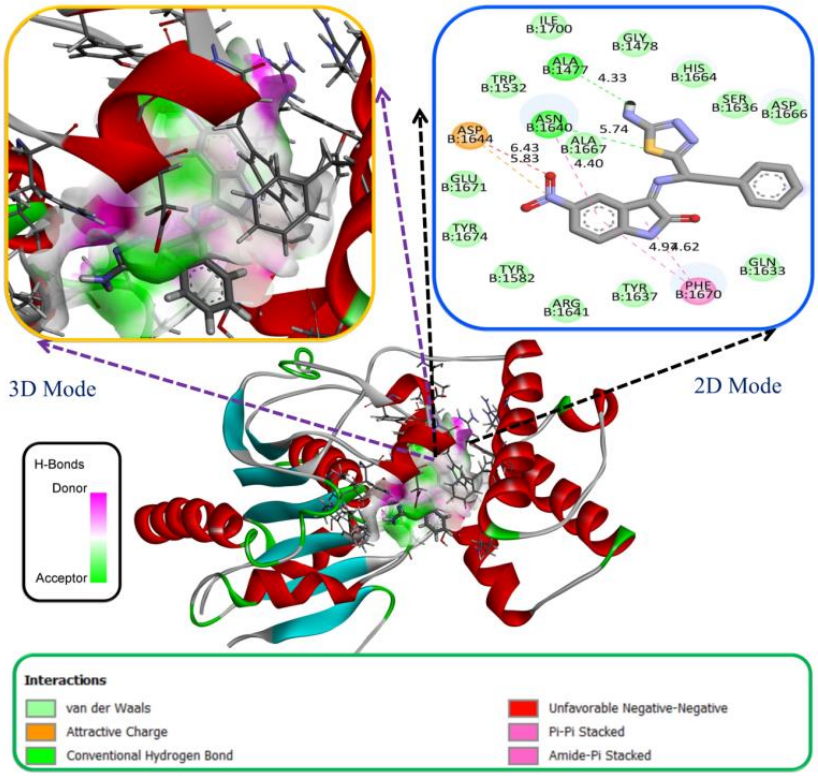

Figure 7. Ligand-5V3Y mode of interaction with enzymes; 3D view of the donor/acceptor surface of hydrogen bonds on the receptor and 2D view of ligand enzyme interactions

3.8. ADME Analysis

ADME studies are now used in medication manufacture to choose the most appealing substances and reduce the danger of drug end-stage attrition. Many characteristics were explored virtually in this study, including drug solubility S, molecular characteristics, cell permeability, HIA, polar surface area PSA, and drug similarity score (Kassel, 2004). These ADME descriptive properties were estimated for compounds of biological relevance and compared to typical medication ranges (Ekins et al., 2006). The synthesized molecules comply with Lipinski's five rule in terms of oral bioavailability and character, which increases their chances of being evaluated as future therapeutic candidates. The estimated Caco 2 permeability and BBB coefficient (log BB) were utilized to determine the overall distribution of chemicals in the human body, and the resulting BBB values were

determined to be acceptable. Table 7 shows the ADME characteristics for the produced compounds. ATSB molecule's toxicity is assessed using fatal dosages and the spectrum of action on various organs and tissues. Online servers such as SwissADME (http://www.swissadme.ch/index.php) have been used. Table 7 demonstrates that ATSB molecule are coherent with MA 394.41 g/mol (<500), LogP values 1.63 (<5), and acceptor hydrogen bond (AHB) 6 (<10) based on Lipinski's rule. The topological PSA values are 167.32. A2 ABS is 51.27%. The physicochemical properties, color spaces, and structure of our study molecule are shown in Figure 8.

Table 7. Physicochemical and lipophilicity of ATSB molecule

Code	Lipophilicity consensus log P	Physico-chemical properties								
ATSB Molecule		MW[a] g/mol	Heavy Atoms	Aromatic heavy atoms	Rot. bond	H-acceptor bond	H-donor bond	MR[b]	TPSA[c] (A^2)	% ABS[d]
	1.63	394.41	28	17	5	6	2	110.70	167.32	51.27

[a]**MW**, molecular weight; [c]**TPSA**, topological polar surface area; [b]**MR**, molar refractivity; [d]**ABS%:** absorption percent $ABS\% = 109 - [0.345 \times TPSA]$.

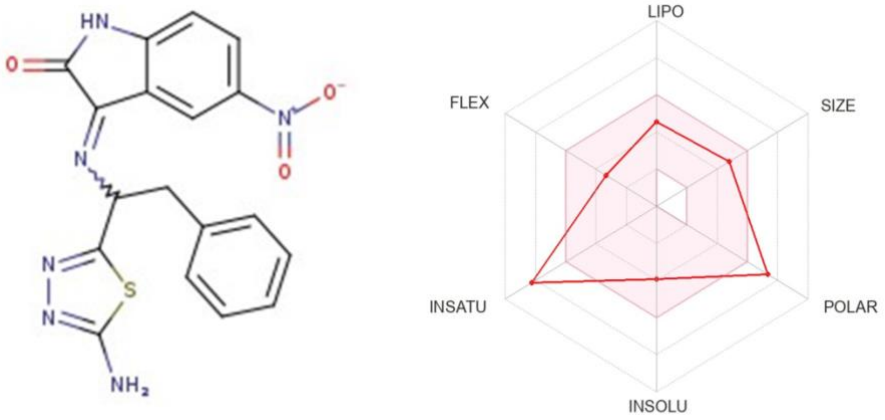

Figure 8. Color regions and physicochemical parameters of ATSB molecule

4. Conclusion

As a result, docking software users must continuously remind themselves of one caution: Analyze their embedded models skeptically. ATSB molecule was originally sketched in ChemBioDraw for DFT calculations in the Gaussian09 software under the theoretical research and results section. The minimized molecules were fed into the Gaussian 09 software, and the structure was subjected to DFT calculations (HOMO-LUMO, geometry optimization, MEPS maps, dipole moment calculations, NBO analysis, and Mulliken Atomic Charges). Our chemical was tested for antibacterial activity as well as antituberculosis activity in vitro. The binding affinity of ligands docked against protein 5V3X was -7.866 Kcal/mol and -8.780 Kcal/mol for docked against protein 5V3Y. In addition, ADME analysis for ATSB molecule was done in this section, and the color zones

are displayed separately. The title compounds from the in silico analysis were found to meet the ADME studies as well as Lipinski's five conditions. Finally, docking experiments for ATSB molecule for two distinct enzymes were performed, and docking scores and receptor models were provided.

Acknowledgements

This section is where one can acknowledge and thank the individuals and/or institutions who helped with and supported the author(s) with her/his/their research.

Authors' Contributions

All authors contributed equally to the study

Statement of Conflicts of Interest

There is no conflict of interest between the authors.

Statement of Research and Publication Ethics

The author declares that this study complies with Research and Publication Ethics.

References

Bagayoko, D. (2014). Understanding density functional theory (DFT) and completing it in practice. *AIP Advances*, *4*(12).

Bağlan, M., Gören, K., & Çakmak, İ. (2022). Theoretical Investigation of ^{1}H and ^{13}C NMR Spectra of Diethanol Amine Dithiocarbamate RAFT Agent [Dietanol Amin Ditiyokarbamat RAFT Ajanının 1H ve 13C NMR Spektrumlarının Teorik İncelenmesi]. *Journal of the Institute of Science and Technology*, *12*(3), 1677-1689.

Bağlan, M., Gören, K., & Yildiko, Ü. (2023a). DFT Computations and Molecular Docking Studies of 3-(6-(3-aminophenyl)thiazolo[1,2,4]triazol-2-yl)-2H-chromen-2-one(ATTC) Molecule. *Hittite Journal of Science and Engineering*, *10*(1), 11-19.

Bağlan, M., Gören, K., & Yildiko, Ü. (2023b). HOMO–LUMO, NBO, NLO, MEP analysis and molecular docking using DFT calculations in DFPA molecule. *International Journal of Chemistry and Technology*, *7*(1), 38-47.

Bağlan, M., Yildiko, Ü., & Gören, K. (2022). Computational Investigation of trihydroxy-3,7-dimethoxy;-O-biflavone from Flavonoids Using DFT Calculations and Molecular Docking. *Adıyaman University Journal of Science*, *12*(2), 283-298.

Bağlan, M., Yildiko, Ü., & Gören, K. (2023). DFT Calculatıons and Molecular Dockıng Study in 6-(2"-Pyrrolıdınone-5"-Yl)-(-) Epıcatechın Molecule from Flavonoıds [Flavonoİdlerden 6-(2"-pyrolİdİnone-5"-yl)-(-)epİcatechİn molekÜlÜnde dft hesaplamalari ve molekÜler yerleŞtİrme ÇaliŞmasi]. *Eskişehir Teknik Üniversitesi Bilim ve Teknoloji Dergisi B - Teorik Bilimler*, *11*(1), 43-55.

Bhuiyan, M. D. H., Ashraf, M., Teshome, A., Gainsford, G. J., Kay, A. J., Asselberghs, I., & Clays, K. (2011). Synthesis, linear & non linear optical (NLO) properties of some indoline based chromophores. *Dyes and Pigments*, *89*(2), 177-187.

Cordes, E. H., & Jencks, W. P. (1962). On the Mechanism of Schiff Base Formation and Hydrolysis. *Journal of the American Chemical Society*, *84*(5), 832-837.

da Silva, C. M., da Silva, D. L., Modolo, L. V., Alves, R. B., de Resende, M. A., Martins, C. V. B., & de Fátima, Â. (2011). Schiff bases: A short review of their antimicrobial activities. *Journal of Advanced Research*, *2*(1), 1-8.

Demir, P., & Akman, F. (2017). Molecular structure, spectroscopic characterization, HOMO and LUMO analysis of PU and PCL grafted onto PEMA-co-PHEMA with DFT quantum chemical calculations. *Journal of Molecular Structure*, *1134*, 404-415.

Ekins, S., Bugrim, A., Brovold, L., Kirillov, E., Nikolsky, Y., Rakhmatulin, E., Sorokina, S., Ryabov, A., Serebryiskaya, T., Melnikov, A., Metz, J., & Nikolskaya, T. (2006). Algorithms for network analysis in systems-ADME/Tox using the MetaCore and MetaDrug platforms. *Xenobiotica*, *36*(10-11), 877-901.

Glendening, E. D., Landis, C. R., & Weinhold, F. (2013). NBO 6.0: Natural bond orbital analysis program. *Journal of Computational Chemistry*, *34*(16), 1429-1437.

Hodnett, E. M., & Dunn, W. J. (1970). Structure-antitumor activity correlation of some Schiff bases. *Journal of Medicinal Chemistry*, *13*(4), 768-770.

Jakhar, R., Dangi, M., Khichi, A., & Chhillar, A. K. (2020). Relevance of Molecular Docking Studies in Drug Designing. *Current Bioinformatics*, *15*(4), 270-278.

Kassel, D. B. (2004). Applications of high-throughput ADME in drug discovery. *Current Opinion in Chemical Biology*, *8*(3), 339-345.

Kurt, M., Babu, P. C., Sundaraganesan, N., Cinar, M., & Karabacak, M. (2011). Molecular structure, vibrational, UV and NBO analysis of 4-chloro-7-nitrobenzofurazan by DFT calculations. *Spectrochimica Acta Part A: Molecular and Biomolecular Spectroscopy*, *79*(5), 1162-1170.

Lakshminarayanan, S., Jeyasingh, V., Murugesan, K., Selvapalam, N., & Dass, G. (2021). Molecular electrostatic potential (MEP) surface analysis of chemo sensors: An extra supporting hand for strength, selectivity & non-traditional interactions. *Journal of Photochemistry and Photobiology*, *6*, 100022.

Metzler, C. M., Cahill, A., & Metzler, D. E. (1980). Equilibriums and absorption spectra of Schiff bases. *Journal of the American Chemical Society*, *102*(19), 6075-6082.

Michael J. Frisch, T., G.W, Bernhard Schlegel, Gustavo Scuseria. (2016). (Version In Revision E.01)

Morris, G. M., & Lim-Wilby, M. (2008). Molecular Docking. In A. Kukol (Ed.), *Molecular Modeling of Proteins* (pp. 365-382). Humana Press. https://doi.org/10.1007/978-1-59745-177-2_19

Prasad, S. R., Satyanarayan, N. D., Shetty, A. S. K., & Thippeswamy, B. (2022). Synthesis, antimicrobial, and antitubercular evaluation of new Schiff bases with in silico ADME and molecular docking studies. *European Journal of Chemistry*, *13*(1), 109-116.

Rodney, D., Ventelon, L., Clouet, E., Pizzagalli, L., & Willaime, F. (2017). Ab initio modeling of dislocation core properties in metals and semiconductors. *Acta Materialia*, *124*, 633-659.

Suhasini, M., Sailatha, E., Gunasekaran, S., & Ramkumaar, G. R. (2015). Vibrational and electronic investigations, thermodynamic parameters, HOMO and LUMO analysis on Lornoxicam by density functional theory. *Journal of Molecular Structure*, *1100*, 116-128.

Taylor, J., Guo, H., & Wang, J. (2001). Ab initio modeling of open systems: Charge transfer, electron conduction, and molecular switching of a ${\mathrm{C}}_{60}$ device. *Physical Review B*, *63*(12), 121104.

Wang, Z., Zhang, W., & Liu, B. (2021). Computational Analysis of Synthetic Planning: Past and Future. *Chinese Journal of Chemistry*, *39*(11), 3127-3143.

Weinhold, F., Landis, C. R., & Glendening, E. D. (2016). What is NBO analysis and how is it useful? *International Reviews in Physical Chemistry*, *35*(3), 399-440.

Yildiko, Ü., Türkan, F., Tanriverdi, A. A., Ata, A. C., Atalar, M. N., & Cakmak, İ. (2021). Synthesis, enzymes inhibitory properties and characterization of 2- (bis (4-aminophenyl) methyl) butan-1-ol compound: Quantum simulations, and in-silico molecular docking studies. *Journal of the Indian Chemical Society*, *98*(11), 100206.